



Published in final edited form as:

Appl Surf Sci. 2017 January 15; 392: 950–959. doi:10.1016/j.apsusc.2016.07.004.

Effect of substrate storage conditions on the stability of “Smart” films used for mammalian cell applications

Blake M. Bluestein, Jamie A. Reed, and Heather E. Canavan*

Center for Biomedical Engineering, Department of Chemical and Biological Engineering, University of New Mexico, United States

Abstract

When poly(*N*-isopropyl acrylamide) (pNIPAM) is tethered to a surface, it can induce the spontaneous release of a sheet of mammalian cells. The release of cells is a result of the reversible phase transition the polymer undergoes at its lower critical solution temperature (LCST). Many techniques are used for the deposition of pNIPAM onto cell culture substrates. Previously, we compared two methods of deposition (plasma polymerization, and co-deposition with a sol-gel). We proved that although both were technically appropriate for obtaining thermoresponsive pNIPAM films, the surfaces that were co-deposited with a sol-gel caused some disruption in cell activity. The variation of cell behavior could be due to the delamination of pNIPAM films leaching toxic chemicals into solution. In this work, we assessed the stability of these pNIPAM films by manipulating the storage conditions and analyzing the surface chemistry using X-ray photoelectron spectroscopy (XPS) and contact angle measurements over the amount of time required to obtain confluent cell sheets. From XPS, we demonstrated that ppNIPAM (plasma polymerized NIPAM) films remains stable across all storage conditions while sol-gel deposition show large deviations after 48 h of storage. Cell response of the deposited films was assessed by investigating the cytotoxicity and biocompatibility. The 37°C and high humidity storage affects sol-gel deposited films, inhibiting normal cell growth and proper thermoresponse of the film. Surface chemistry, thermoresponse and cell growth remained similar for all ppNIPAM surfaces, indicating these substrates are more appropriate for mammalian cell culture applications.

Keywords

pNIPAM; Isopropyl acrylamide; XPS; ESCA; Mammalian cells

1. Introduction

Poly(*N*-isopropyl acrylamide), or pNIPAM, is a commonly used thermoresponsive biocompatible polymer [1–11]. It is significant for the biomedical engineering community due to the polymer’s unique ability to change its wettability near physiological temperatures [12]. Above the lower critical solution temperature (LCST), which is ~32°C, the polymer is relatively hydrophobic, causing it to collapse when it is tethered to a surface. In this state,

*Corresponding author at: University of New Mexico, MSC01 1141, Albuquerque, New Mexico 87131, United states. Canavan@unm.edu (H.E. Canavan).

cells will readily attach and proliferate on these surfaces in a manner similar to how they behave on traditional cell culture substrates. Below the LCST, near room temperature (25°C), the polymer becomes relatively hydrophilic [3,6,13,14]. In this swollen state, cells spontaneously detach from the substrate as a confluent sheet [10,15,16]. This form of detachment has made pNIPAM popular for cell sheet engineering and other biological applications, as reviewed by Cooperstein et al. [17].

To date, pNIPAM films have been used for a number of clinical applications in many countries around the world, including corneal and cardiac implants in Japan [18–23]. However, development has been limited in the United States of engineered tissues from cell sheets harvested with pNIPAM for clinical applications due to an uncertainty of the mechanism behind the cell release [24–26]. Currently, it is unknown if pNIPAM detaches from the underlying substrate and is transferred with the cells upon cell detachment, which would raise concern as to whether pNIPAM is biocompatible [24]. Most of the research performed on the polymer focuses on the material characteristics, but do not assess the biocompatibility of the tethered polymer. In fact, there are very few studies on the cytotoxicity of pNIPAM. Furthermore, the few studies that do exist, report conflicting conclusions [1,8,9,11,27–43]. One thing that is clear is that the monomer is toxic [44]. Thus, if there were any uncrosslinked monomer remaining in a pNIPAM film, the monomer may be able to leach into the surrounding cellular environment causing cytotoxicity. Therefore, any instability of a pNIPAM film could lead to cytotoxicity, thus the method of deposition could affect the biocompatibility.

There are many methods for depositing pNIPAM onto a substrate, including atom transfer radical polymerization (ATRP), electron beam ionization, and solution deposition [14,35,41,45–47]. Previously, we compared two methods of deposition (plasma and co-deposition with a sol-gel), demonstrating that both were technically appropriate for obtaining thermoresponsive pNIPAM films. However, the surfaces that were co-deposited with a sol-gel seemed to cause some disruption in cell activity [48]. In that work, we concluded that the cell behavior variation could be due to film instability and delamination, causing chemicals to leach out from the surface. Takezawa et al. have previously stored their surfaces below the LCST before use, to ensure film stability [50].

This study investigates the stability of both plasma polymerized and sol-gel co-deposited pNIPAM substrates for the amount of time required to obtain confluent cell sheets. As the ultimate goal is to use these substrates as cell culture platforms and thus film stability is required, we have also investigated claims that the conditions of surface storage, thus the initial conformation of the polymer when exposed to cell growth media and cells, affect the stability of pNIPAM films during cell culture. Therefore, we will further investigate the two methods of deposition to determine if there is film instability and if this instability can be avoided by altering the storage of the films pre-cell culture by assessing film chemistry, thermoresponse, cytotoxicity, and biocompatibility.

2. Experimental methods

Round glass cover slips (15 mm) were purchased from Ted Pella, Inc. (Redding, CA). The silicon chips were obtained from Silitec (Salem, OR). The 200 proof ethanol, HPLC grade methanol, HPLC grade dichloromethane and hydrochloric acid were purchased from Honeywell Burdick & Jackson (Deer Park, TX). The acetone was purchased from Fisher Scientific (Pittsburgh, PA).

The cell culture media was from Hyclone (Logan, UT). Bovine aortic endothelial cells (BAECs) were from Genlantis (San Diego, CA) and cultured in 24 well tissue culture polystyrene (TCPS) plates from Greiner Bio-one (Monroe, NC) and in 96 well TCPS plates from Corning Incorporated (Corning, NY). The DPBS without calcium-chloride or magnesium-chloride was purchased from HyClone (Logan, UT). The 0.25% trypsin-EDTA was from Gibco (Carlsbad, CA).

Statistically relevant data were obtained by repeating all procedures three times. Each replication of the experiment used three surfaces, with each surface analyzed in three different sites along the surface. This method was used for both surface analysis and cell behavior studies.

2.1. Surface preparation

Glass cover slips used for cell culture were cleaned with an acid wash (1:1 vol HCl:MeOH), rinsed with deionized water, and dried with nitrogen. Silicon chips used for surface analysis were washed with 10-min intervals in dichloromethane, acetone, and then methanol in an ultrasonic cleaner from VWR International (Brisbane, CA).

2.2. spNIPAM preparation and deposition

The pNIPAM (molecular weight of ~40,000) was purchased from Polysciences, Inc (Warrington, PA). The tetraethyl orthosilicate (TEOS) was purchased from Sigma-Aldrich (St. Louis, MO). Sample preparation was presented by Reed et al. [13]. Briefly, a solution of pNIPAM (35 mg of pNIPAM, 5 mL of distilled water, and 200 μ L of 1 N HCl) and a sol-gel mixture (250 μ L TEOS sol (1 TEOS:3.8 ethanol:1.1 water:0.0005 HCl), 43 μ L distilled water, 600 μ L ethanol) were mixed to obtain 0.35 wt% pNIPAM in solution.

100–200 μ L of the prepared solution was evenly distributed on clean surfaces placed on a spin coater, model 100 spinner from Brewer Science, Inc. (Rolla, MO). These surfaces were then spun at 2000 rpm for 60 s. The surfaces were stored under nitrogen in a Parafilm covered Petri dish.

2.3. PpNIPAM preparation and deposition

Plasma polymerization was described previously by Lucero et al. [51]. Briefly, the deposition was performed in a reactor chamber fabricated to our design specifications by Scientific Glass (Albuquerque, NM). *N*-isopropyl acrylamide (99%) was purchased from Acros Organics (Geel, Belgium). To spark a plasma in the chamber, two 2.5 cm copper electrodes are connected to a Dressler (Stolberg, Germany) matching network and radio frequency (RF) power generator. An argon etch and a methane adhesion promoting layer

was deposited prior to pNIPAM deposition. During pNIPAM deposition, the power setting of the RF generator is slowly decreased from 100W to 0W over 35 min manually: at 100W for 5 min, 10W for 5 min, 5W for 5 min, 1W for 10 min, and 0W for 10 min.

After the samples are removed from the reactor, they are rinsed with cold DI water to remove any uncrosslinked NIPAM off of the surface, and dried with nitrogen. The surfaces are placed in a Petri dish, backfilled with nitrogen, and sealed with Parafilm.

2.4. Storage of surfaces

After modification the surfaces were stored at 25°C with low humidity conditions (30% relative humidity), 25°C with high humidity conditions (90% relative humidity), 37°C with low humidity conditions, or 37°C with high humidity conditions. Surfaces were stored in these conditions for at least 24 h before use.

2.5. Contact angles

An Advanced Goniometer model 300-UPG (ramé-hart instrument co., Mountain Lakes, NJ) with an environmental chamber and DROPimage Standard program was used to measure inverted bubble contact angles in Ultrapure water (18 MΩ). Contact angles were taken at room temperature and 37°C using the Temp Controller model 100–500 connected to the environmental chamber.

2.6. X-ray photoelectron spectroscopy (XPS)

All XPS spectra were obtained using a Kratos Axis-Ultra DLD spectrometer. This instrument has a monochromatized Al K α X-ray and a low energy electron flood gun for charge neutralization. X-ray spot size for these acquisitions was on the order of 300 \times 700 μ m (Kratos 'Hybrid' mode). Pressure in the analytical chamber during spectral acquisition was $\sim 5 \times 10^{-9}$ Torr. Pass energy for survey spectra was 80 eV and the pass energy was 20 eV for high-resolution spectra (carbon).

Data treatment was performed on CasaXPS software (Manchester, UK). Core-level spectra were peak fit using the minimum number of peaks possible to obtain random residuals. A 70% Gaussian/30% Lorentzian line shape was used to fit the peaks, and a linear function was used to model the background.

2.7. Cell culture

BAECs were cultured in Dulbecco's Modified Eagle Medium supplemented with 10% fetal bovine serum, 1% penicillin/streptomycin, 4.5 g/L glucose, 0.1 mM MEM nonessential amino acids, and 1 mM MEM sodium pyruvate. Cells were incubated at 37°C in a humid atmosphere with 5% CO₂. Cells were washed with Dulbecco's phosphate buffered saline and lifted from culture flasks with 0.25% trypsin to seed 24 well plates with inserted pNIPAM deposited and blank control cover glass.

2.8. Substrate cytotoxicity

To determine if the substrates were leaching any cytotoxic material, they were incubated at cell culture conditions with 3 mL/cm³ media for 24 h [52]. This treated media was used to

replace media on BAECs at 60% confluence and the cells were incubated with the treated media for 24 h, at which point any cytotoxic material would have affected the growth and viability of the cells. The cells were incubated with 100%, 10%, 1%, and 0% treated media. To analyze the cells' viability, we used a LIVE/DEAD[®] staining kit from Invitrogen (Carlsbad, CA) and imaged with a 20× objective using a fluorescent microscope (Nikon F100, Melville, NY).

2.9. Biocompatibility

BAECs were seeded at a low density (~15,000 cells/well) and incubated for 6 h, 24 h, and 72 h [52]. At each of these time points the cells were imaged using bright field microscopy, followed by analyzing the cells' viability using a LIVE/DEAD[®] staining kit from Invitrogen (Carlsbad, CA) and imaged with a 20× objective using a fluorescent microscope (Nikon F100, Melville, NY).

2.10. Delamination study

Coated silicon chips were used for surface analysis. These surfaces were submerged in DPBS for 2 h and 48 h to compare to cell response. Each silicon chip was rinsed thoroughly with Ultrapure water (18 MΩ) and dried with nitrogen after submersion in DPBS.

3. Results

3.1. Initial conditions

Using XPS, it was confirmed that there was successful deposition of pNIPAM using both the spNIPAM and ppNIPAM deposition methods. As demonstrated by the relative atomic percentages in Table 1, before submerging the surfaces in DPBS, all surfaces are relatively similar to the theoretical values (75% C, 12.5% O, and 12.5% N) calculated from the composition of the monomer. It should be noted that spNIPAM surfaces differed from theoretical values due to the presence of Si at 7–20%, which arises from the use of TEOS sol. In addition, pure pNIPAM would be composed of 66.7% CH/CC (285 eV), 16.7% amide (286 eV), and 16.7% amine (288 eV) bonds. The high resolution C1s spectra in Fig. 1 and the data in Table 2 illustrates that spNIPAM (68.7% CH/CC, 17.1% amide, and 14.2% amine) and ppNIPAM (62.1% CH/CC, 20.8% amide, and 17.1% amine) surfaces have similar bonding environments to the theoretical values, as demonstrated previously, proving deposition of pNIPAM in each case. [13,51,53]

Using contact angle goniometry, it was confirmed that the surfaces, prior to exposure to DPBS, were thermoresponsive (see Table 3). The thermoresponse at 0 h for both ppNIPAM and spNIPAM at all temperatures and relative humidity values follow the desired trend of higher contact angles above the LCST and lower contact angles below the LCST. PpNIPAM surfaces stored at 25°C with low humidity change in contact angle across the LCST (~17°, with the standard deviation for all ppNIPAM contact angles at 0 h < 3.0°). While spNIPAM surfaces had a 6.4° change in contact angle (standard deviation for all spNIPAM contact angles at 0 h are < 2.5°). The control surfaces stored at 25°C with low humidity showed no statistical change across the LCST; as expected, the controls followed this trend throughout the experiment irrespective of storage temperatures and relative humidity values. The

controls did exhibit an increase in hydrophilicity after storage in DPBS for 48 h, due to a film of trace salts. However, the surfaces were not thermoresponsive across the LCST.

With a shift to a higher relative humidity, ppNIPAM surfaces are still thermoresponsive, although the change in the contact angle across the LCST decreased compared to 0 h (7.7° vs 17° respectively). This could be due to increased incorporation of water in the film when stored at high humidity conditions. The spNIPAM surfaces remained relatively stable with a 6.3° change. When the temperature was shifted to 37°C at low humidity, ppNIPAM surfaces exhibited about a 5.9° change in contact angle, and spNIPAM exhibited a 9.3° change in contact angle. At 37°C ppNIPAM and spNIPAM surfaces remained stable with 8.7° and 9.1° changes in contact angle respectively when the humidity value was shifted to a higher relative humidity (N = 9, with a standard deviation of less than three except for those marked in Table 3 by an asterisk which has a standard deviation of less than five). This indicates that although the surfaces were all stored at different temperatures and relative humidity conditions, the surfaces had a 5°–10° change in contact angle before submersion in DPBS, with thermoresponse that is similar to what has been previously reported [24,48]. It has been found by Cole et. al that for contact angles, the relative difference is more important than the absolute value in determining stability and tissue engineering compatibility [49]. Similar results were found in our study.

3.2. Surface stability

Over the 48 h period necessary to obtain confluent cell sheets, ppNIPAM surfaces appear chemically stable, showing no statistically relevant deviation in relative atomic percentage of species present initially (62.1% C, 20.8% N, and 17.1% O) regardless of the storage conditions. In addition, high resolution C1s spectra indicate that carbon species present also remained statistically unchanged, despite the storage condition or time exposed to DPBS (see Fig. 1 and Table 2).

The relative humidity of the storage condition has very little influence on surface chemistry, as illustrated by the lack of change on spNIPAM films that were highly influenced by temperature. Above the LCST, regardless of humidity, the surface chemistry of spNIPAM films begin to deviate from the theoretical pNIPAM with a 5.0% and 12.3% increase in Si and O₂ and a 14.6% and 2.7% decrease in C and N respectively. This indicates that the pNIPAM may be delaminating from the surface, and there is more TEOS than pNIPAM present on the surface. Below the LCST, a similar trend is seen with a decrease in 5.2% C and a 4.3% increase in Si, but there is not statistically relevant shifts in O or N.

PpNIPAM surfaces retained a 5°–12° change in contact angle across the LCST, the largest change in contact angle was observed with the ppNIPAM films stored at 25°C with low relative humidity. As importantly, there was no statistical difference in thermoresponse seen by changing the storage conditions of the ppNIPAM surfaces.

The results also show that the thermoresponse for ppNIPAM films were most affected by humidity, while spNIPAM films were affected by storage temperature. Furthermore, the best thermoresponse was seen on ppNIPAM surfaces that were stored at 25°C and low humidity. Obviously, these results indicate that temperature is affecting the stability of the films. In

contrast, Takezawa et al., found that their pNIPAM films are more stable when stored below the LCST (it should be noted that humidity was not a variable for their experiments) [50].

In contrast, the spNIPAM surfaces appear to lose the thermoresponsive characteristic of pNIPAM regardless of storage conditions. In fact, at the time when these surfaces would need to be thermoresponsive to obtain cell sheet release (2 days), the surfaces have reversed thermoresponse (a -6° – 0° change). As early as 2 h after submersion in DPBS, the surfaces have drastically reduced thermoresponse, dropping from a 6° – 9° change to a 2° – 6° change. These results indicate that there is a change in the spNIPAM films' characteristics almost immediately, possibly due to the delamination of the film.

From these results, it appears that ppNIPAM surfaces remain stable chemically and maintain thermoresponse during the experimental time frame that is consistent with cell culture. This would suggest that the ppNIPAM surfaces should have a better cell detachment than the spNIPAM surfaces. However, as determined by Lucero, et al. thermoresponse is not always a reliable indicator of cell response [51].

3.3. Cell adhesion

BAECs were cultured using previously described technique. [16] Cells attached to ppNIPAM surfaces within 2 h of seeding, comparable to blank control surfaces. However, images obtained 2 h after seeding the cells indicate that the cells are less likely to attach to spNIPAM surfaces stored below the LCST initially (see Fig. 2, middle row). Eventually, cells grew to confluence on all surfaces, suggesting that deposition and storage method do not affect the long-term cell growth of the surfaces. Since the cells do ultimately attach to the surfaces (as shown in Fig. 3), and surface analysis suggests that there is delamination, the cells are most likely attaching post delamination for all surfaces except those stored above the LCST in low humidity conditions. In this case, there is still limited cell attachment with many cell aggregates, indicating that these adherent cells would rather attach to each other than the substrate. Due to the aforementioned lack of cell attachment, the viability of the cells on the surfaces was analyzed.

3.4. Cytotoxicity

A cytotoxicity study was completed to investigate the effect of the pNIPAM leaching into the media. This was done by incubating the ppNIPAM and spNIPAM surfaces from each storage condition at cell culture conditions with media for 24 h [52]. Since it was clear from surface analysis that there was delamination of the spNIPAM surfaces, anything that would delaminate from the surfaces would be collected in this treated media. Therefore, if either the spNIPAM or ppNIPAM surfaces are leaching out harmful chemical byproducts to the cells, when the treated media is used during incubation with normal, healthy cells, the cells should no longer be viable. In this case, BAECs were incubated with 100%, 10%, 1%, and 0% treated media to determine if there were any cytotoxic chemicals leaching into the treated media, as well as to determine what amount of the cytotoxic chemicals would decrease cell viability. As shown in Fig. 4, even when healthy cells were incubated with 100% treated media, there was no adverse effect on viability for either spNIPAM or

ppNIPAM surfaces. The cells remained viable, staining green with a LIVE/DEAD[®] assay, with the highest possible amount of the leached chemicals.

3.5. Biocompatibility

Cells were monitored at different time points when cultured directly on the substrates to see which storage conditions would be the most biocompatible, or which surfaces supported cell growth and proliferation. BAECs were seeded at a low density and incubated for 6 h, 24 h, and 72 h. [52] Again, the cells' viability was monitored with a LIVE/DEAD[®] assay to determine whether the cells that were present at each time point were healthy. As previously mentioned, there was minimal cell attachment to the spNIPAM surfaces initially (see Fig. 5). However, after 24 h, all surfaces have some cell attachment and proliferation. At this time point, spNIPAM surfaces were still not as populated compared to ppNIPAM surfaces. The most cell attachment for spNIPAM surfaces at 24 h was on surfaces stored at 37°C, low humidity. These were also the surfaces that had lost all thermoresponse at 2 h, and thus have delaminated to the point that the cells can better anchor to the substrate. By the final time point at 72 h, the cells were most confluent on ppNIPAM substrates previously stored at 25°C, low humidity. As seen in Fig. 5, all surfaces stored at 25°C had increased proliferation than those stored at 37°C, regardless of humidity. However, all surface conditions were technically biocompatible, resulting in eventual cell attachment and proliferation without any cytotoxicity.

These results illustrate that all of the surfaces, including TEOS, regardless of deposition method and storage conditions, are appropriate for mammalian cell culture and cell detachment. Thus, even if the surfaces are delaminating, this is not affecting the growth or viability of the cells. However, since the primary use for these substrates is to generate cell sheets, which require intact pNIPAM films, ppNIPAM surfaces prove to be most useful. In the interest of thoroughness, five cell lines were tested for biocompatibility via culturing them on ppNIPAM films after storage at 25°C with low relative humidity. All five cell lines showed normal adherence and viability. Therefore, ppNIPAM films stored in this manner were biocompatible, and ideal for tissue engineering applications.

4. Conclusions

Although pNIPAM can be deposited using spin coating and plasma deposition, the surfaces are affected by both deposition method and storage condition. Over time, we find the spNIPAM surfaces delaminate, regardless of storage conditions. Interestingly, at temperatures below the LCST, the surfaces begin to resemble pure pNIPAM substrates, while surfaces stored above the LCST quickly lose thermoresponse and chemical environments indicative of a pNIPAM substrate. This delamination also affects cell attachment/detachment, resulting in limited attachment until after a majority of delamination occurs, and the surfaces better resemble their final state. PpNIPAM surfaces are more stable over time, regardless of the storage conditions, these surfaces have more cell attachment, proliferation, and detachment than the spNIPAM surfaces, making them more useful for cell sheet engineering applications. In addition, storage below the LCST creates more stable surfaces for mammalian cell applications. Although humidity seems to only slightly affect

surface chemistry, thermoresponse, and cell studies for ppNIPAM surfaces, there is a slight preference of cells to surfaces stored in low humidity conditions.

Acknowledgments

The authors would like to thank, Kieran Gallagher-Gonzales, Adrienne Lucero, Xunpei Liu, Phuong Nguyen, and Steven Candelaria for their contributions and helpful discussions. We also thank Lara Gamble and Jim Hull from the National ESCA and Surface Analysis Center for Biomedical Problems (NESAC/BIO) for data acquisition.

This work was funded by NSF-Partnerships for Research and Education in Materials (PREM) program grant # DMR-0611616, NIBIB grant EB-002027, as well as funding from 3M Corporation and the UNM Center for Biomedical Engineering.

JAR was funded by the NSF Graduate Research Fellowship Program and the NIH Ruth Kirschstein National Research Service Award.

References

1. Bisht HS, Manickam DS, You YZ, Oupicky D. *Biomacromolecules*. 2006; 7(4):1169–1178. [PubMed: 16602735]
2. Fukumori K, Akiyama Y, Kumashiro Y, Kobayashi J, Yamato M, Sakai K, Okano T. *Macromol. Biosci.* 2010; 10(10):1117–1129. [PubMed: 20503196]
3. Kumashiro Y, Yamato M, Okano T. *Ann. Biomed. Eng.* 2010; 38(6):1977–1988. [PubMed: 20387117]
4. Takahashi H, Nakayama M, Yamato M, Okano T. *Biomacromolecules*. 2010; 11(8):1991–1999. [PubMed: 20593758]
5. Tang ZL, Akiyama Y, Yamato M, Okano T. *Biomaterials*. 2010; 31(29):7435–7443. [PubMed: 20647153]
6. Canavan HE, Cheng XH, Graham DJ, Ratner BD, Castner DG. *Plasma Processes Polym.* 2006; 3(6–7):516–523.
7. Ista LK, Mendez S, Lopez GP. *Biofouling*. 2009; 26(1):111–118.
8. Lu HF, Targonsky ED, Wheeler MB, Cheng YL. *Biotechnol. Bioeng.* 2007; 96(1):146–155. [PubMed: 16894633]
9. Qin J, Jo YS, Ihm JE, Kim DK, Muhammed M. *Langmuir*. 2005; 21(20):9346–9351. [PubMed: 16171372]
10. Schmaljohann D. *E-Polymers*. 2005:21.
11. Zhang HL, Iwama M, Akaike T, Urry DW, Pattanaik A, Parker TM, Konishi I, Nikaido T. *Tissue Eng.* 2006; 12(2):391–401. [PubMed: 16548697]
12. Canavan HE, Cheng XH, Graham DJ, Ratner BD, Castner DG. *J. Biomed. Mater. Res.* 2005; A 1(75 A):1–13.
13. Reed JA, Lucero AE, Hu S, Ista LK, Bore MT, Lopez GP, Canavan HE. *ACS Appl. Mater. Interfaces*. 2010; 2(4):1048–1051. [PubMed: 20423125]
14. Da Silva RMP, Mano JF, Reis RL. *Trends Biotechnol.* 2007; 25(12):577–583. [PubMed: 17997178]
15. Schmaljohann D, Oswald J, Jorgensen B, Nitschke M, Beyerlein D, Werner C. *Biomacromolecules*. 2003; 4(6):1733–1739. [PubMed: 14606903]
16. Reed JA, Lucero AE, Cooperstein MA, Canavan HE. *J. Appl. Biomater. Biomech.* 2008; 6(2):81–88. [PubMed: 20740450]
17. Cooperstein MA, Canavan HE. *Langmuir*. 2010; 26(11):7695–7707. [PubMed: 20496955]
18. Lai JY, Chen KH, Hsiue GH. *Transplantation*. 2007; 84(10):1222–1232. [PubMed: 18049106]
19. Kondoh H, Sawa Y, Miyagawa S, Sakakida S, Memon MA, Kawaguchi N, Matsuura N, Shimizu T, Okano T, Matsuda H. *Cardiovasc. Res.* 2006; 69(2):466–475. [PubMed: 16423569]
20. Miyagawa S, Sawa Y, Sakakida S, Taketani S, Kondoh H, Memon IA, Imanishi Y, Shimizu T, Okano T, Matsuda H. *Transplantation*. 2005; 80(11):1586–1595. [PubMed: 16371930]

21. Shimmura S, Doillon CJ, Griffith M, Nakamura M, Gagnon E, Usui A, Shinozaki N, Tsubota K. *Cornea*. 2003; 22(7):S81–S88. [PubMed: 14703712]
22. Shimizu T, Yamato M, Isoi Y, Akutsu T, Setomaru T, Abe K, Kikuchi A, Umezu M, Okano T. *Circ. Res.* 2002; 90(3):E40–E48. [PubMed: 11861428]
23. Shimizu T, Yamato M, Akutsu T, Shibata T, Isoi Y, Kikuchi A, Umezu M, Okano T. *J. Biomed. Mater. Res.* 2002; 60(1):110–117. [PubMed: 11835166]
24. Canavan HE, Cheng XH, Graham DJ, Ratner BD, Castner DG. *Langmuir*. 2005; 21(5):1949–1955. [PubMed: 15723494]
25. Tunc M, Humayun M, Cheng XH, Ratner BD. *Retina- J. Retinal Vitreous Dis.* 2008; 28(9):1338–1343.
26. Okano T, Yamada N, Okuhara M, Sakai H, Sakurai Y. *Biomaterials*. 1995; 16(4):297–303. [PubMed: 7772669]
27. Cheng H, Zhu JL, Sun YX, Cheng SX, Zhang XZ, Zhuo RX. *Bioconjugate Chem.* 2008; 19(7):1368–1374.
28. Francis MF, Dhara G, Winnik FM, Leroux JC. *Biomacromolecules*. 2001; 2(3):741–749. [PubMed: 11710027]
29. Hsiue GH, Chang RW, Wang CH, Lee SH. *Biomaterials*. 2003; 24(13):2423–2430. [PubMed: 12699680]
30. Hsiue GH, Hsu SH, Yang CC, Lee SH, Yang IK. *Biomaterials*. 2002; 23(2):457–462. [PubMed: 11761166]
31. Le Garrec D, Taillefer J, Van Lier JE, Lenaerts V, Leroux JC. *J. Drug Target*. 2002; 10(5):429–437. [PubMed: 12442814]
32. Li YY, Zhang XZ, Cheng H, Kim GC, Cheng SX, Zhuo RX. *Biomacromolecules*. 2006; 7(11):2956–2960. [PubMed: 17096519]
33. Li YY, Zhang XZ, Cheng H, Zhu JL, Li UN, Cheng SX, Zhuo RX. *Nanotechnology*. 2007; 18(50)
34. Li YY, Zhang XZ, Zhu JL, Cheng H, Cheng SX, Zhuo RX. *Nanotechnology*. 2007; 18(21)
35. Lu XJ, Zhang LF, Meng LZ, Liu YH. *Polym. Bull.* 2007; 59(2):195–206.
36. Matsumaru Y, Hyodo A, Nose T, Ito S, Hirano T, Ohashi S. *J. Biomater. Sci.-Polym. Ed.* 1996; 7(9):795–804. [PubMed: 8773883]
37. Ozyurek Z, Komber H, Gramm S, Schmaljohann D, Muller AHE, Voit B. *Macromol. Chem. Phys.* 2007; 208(10):1035–1049.
38. Reddy TT, Kano A, Maruyama A, Hadano M, Takahara A. *Biomacromolecules*. 2008; 9(4):1313–1321. [PubMed: 18355026]
39. Vihola H, Laukkanen A, Valtola L, Tenhu H, Hirvonen J. *Biomaterials*. 2005; 26(16):3055–3064. [PubMed: 15603800]
40. Wadajkar AS, Koppolu B, Rahimi M, Nguyen KT. *J. Nanopart. Res.* 2009; 11(6):1375–1382.
41. Yim H, Kent MS, Mendez S, Lopez GP, Satija S, Seo Y. *Macromolecules*. 2006; 39(9):3420–3426.
42. Zintchenko A, Ogris M, Wagner E. *Bioconjugate Chem.* 2006; 17(3):766–772.
43. Cooperstein MA, Canavan HE. *Biointerphases*. 2013; 8(19):1–12. [PubMed: 24706114]
44. Senden RJ, De Jean P, McAuley KB, Schreiner LJ. *Phys. Med. Biol.* 2006; 51(14):3301–3314. [PubMed: 16825731]
45. Angiolini L, Benelli T, Giorgini L, Paris F, Salatelli E, Fontana MP, Camorani P. *Eur. Polym. J.* 2008; 44(10):3231–3238.
46. Fu Q, Rao GVR, Ward TL, Lu YF, Lopez GP. *Langmuir*. 2007; 23(1):170–174. [PubMed: 17190500]
47. Winnik FM, Ringsdorf H, Venzmer J. *Macromolecules*. 1990; 23(8):2415–2416.
48. Reed JA, Love SA, Lucero AE, Haynes CL, Canavan HE. *Langmuir*. 2011 submitted.
49. Cole MA, Voelcker NH, Thissen H, Griesser HJ. *Biomaterials*. 2009; 30:1827–1850. [PubMed: 19144401]
50. Takezawa T, Mori Y, Yoshizato K. *Bio-Technology*. 1990; 8(9):854–856. [PubMed: 1366797]
51. Lucero AE, Reed JA, Wu X, Canavan HE. *Plasma Processes Polym.* 2010; 7(12):992–1000.

52. Timmer MD, Shin H, Horch RA, Ambrose CG, Mikos AG. *Biomacromolecules*. 2003; 4:1026–1033. [PubMed: 12857088]
53. Reed JA, Love SA, Lucero AE, Haynes CL, Canavan HE. *Langmuir*. 2011

Author Manuscript

Author Manuscript

Author Manuscript

Author Manuscript

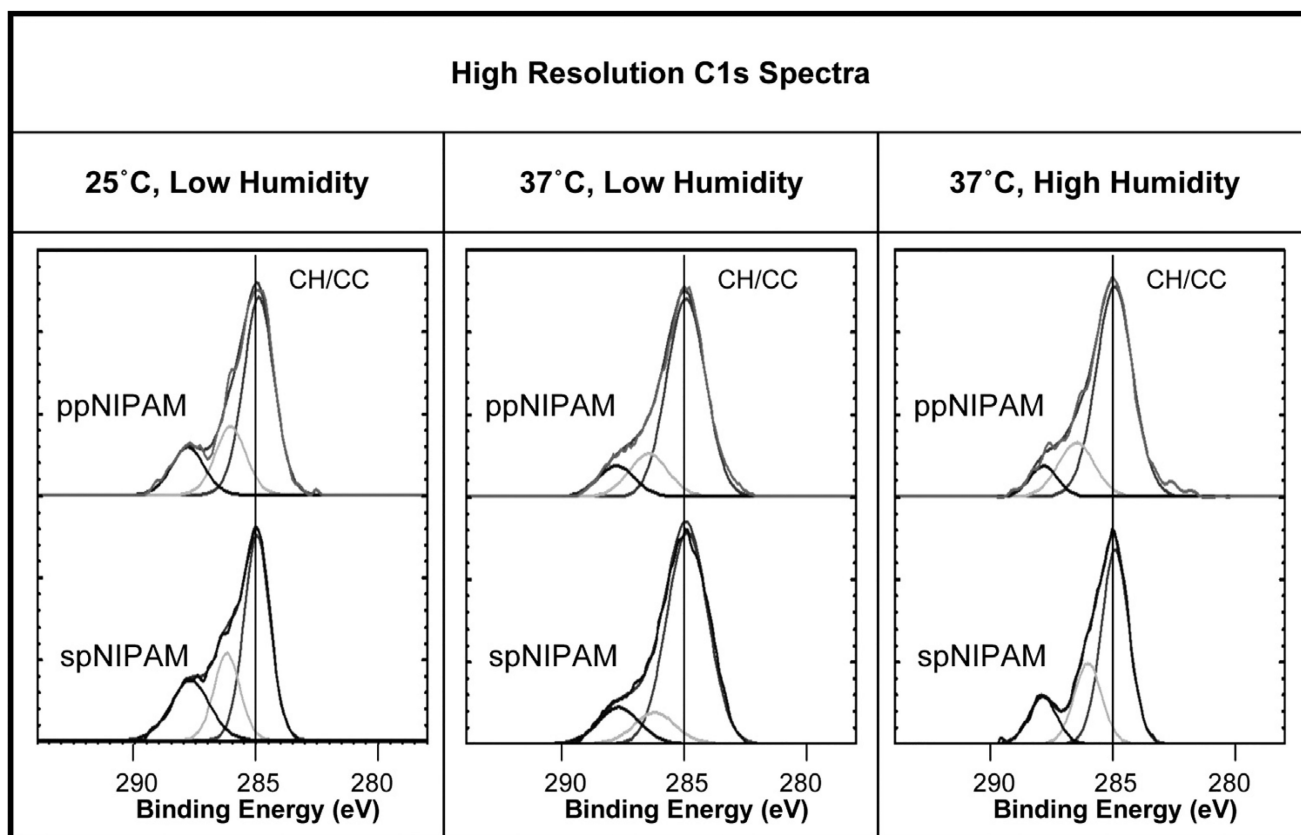


Fig. 1. XPS high resolution C1s spectra of ppNIPAM (top) and spNIPAM (bottom) films after storage in 25°C, low humidity (left) and 37°C low (middle) and high (right) humidity conditions. All surfaces have the bonding environments indicative of pNIPAM deposition, including CH/CC (285 eV), CN/CO (286 eV), and O=CN (288 eV).

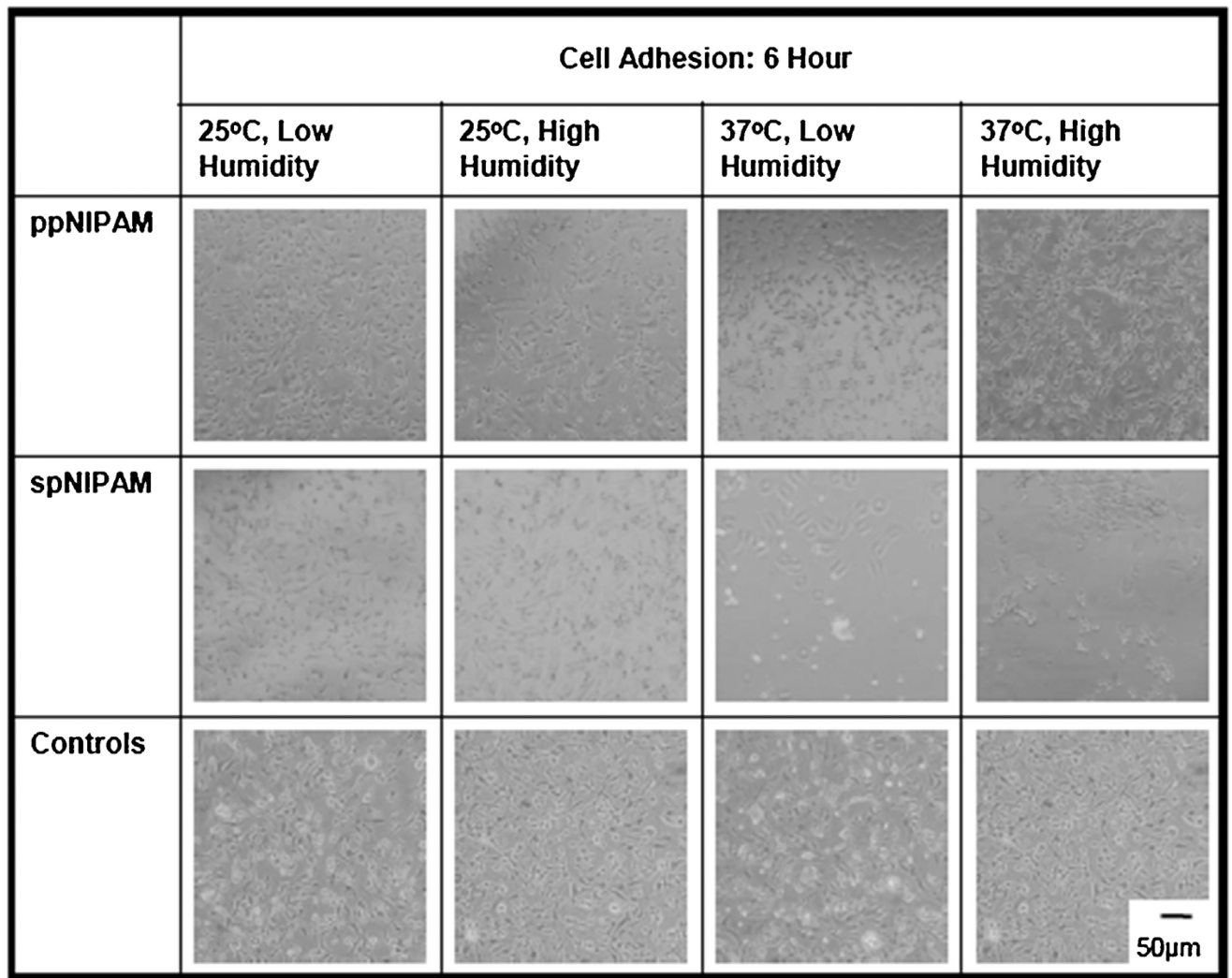


Fig. 2. Bright field microscopy images obtained 6 h prior to cell seeding on ppNIPAM (top), spNIPAM (middle), or blank control glass surfaces (bottom). Within 6 h, there was normal cell attachment onto ppNIPAM and control surfaces, but minimal adhesion to spNIPAM surfaces.

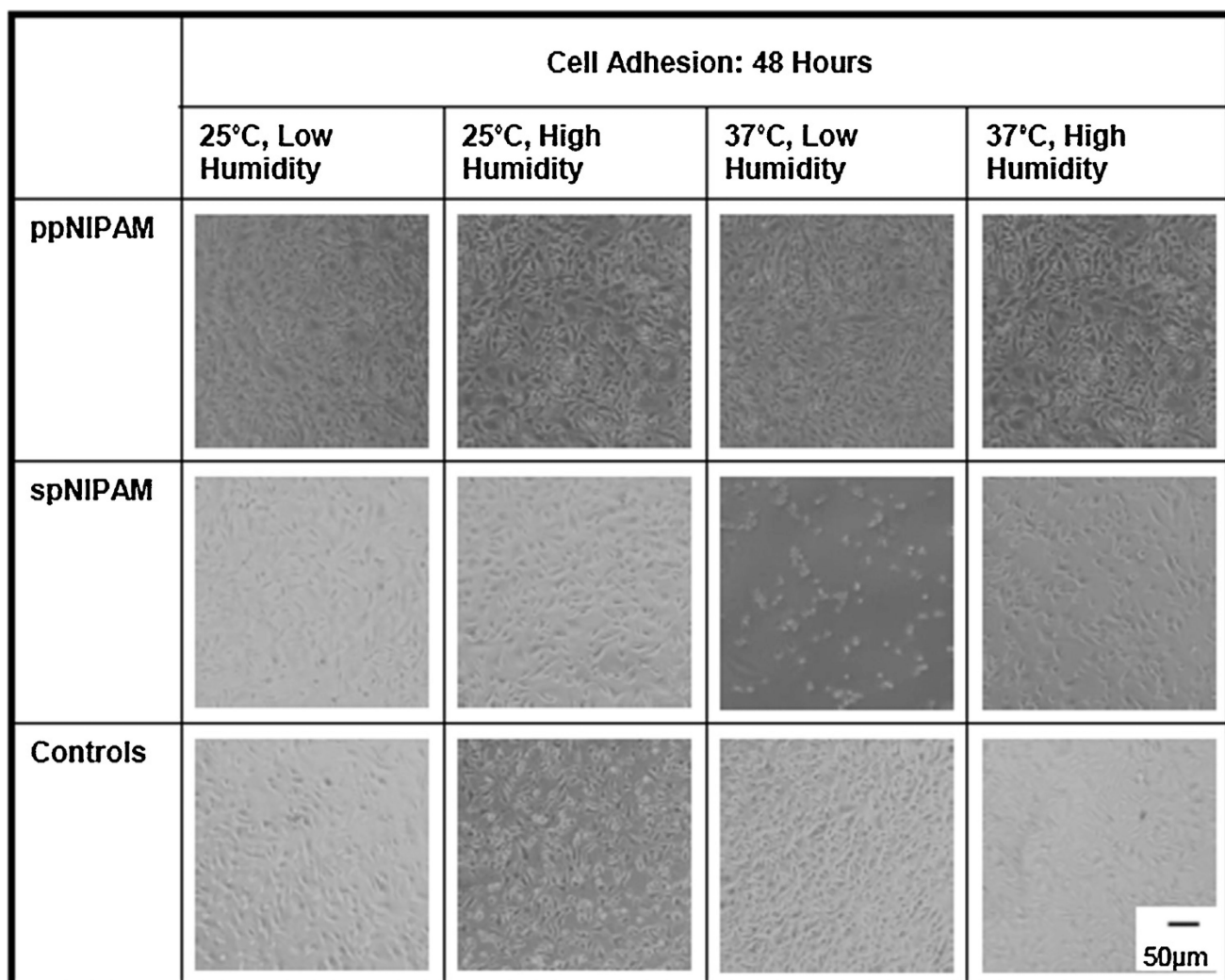


Fig. 3. Bright field microscopy images of BAECs after 48 h of incubation on ppNIPAM, spNIPAM, and control glass surfaces. Cells grown on ppNIPAM grew to confluence within 48 h. However, on spNIPAM surfaces the cells have not reached full confluence on any of the surfaces, where the 37°C low humidity storage conditions for these surfaces demonstrated the least cell attachment.

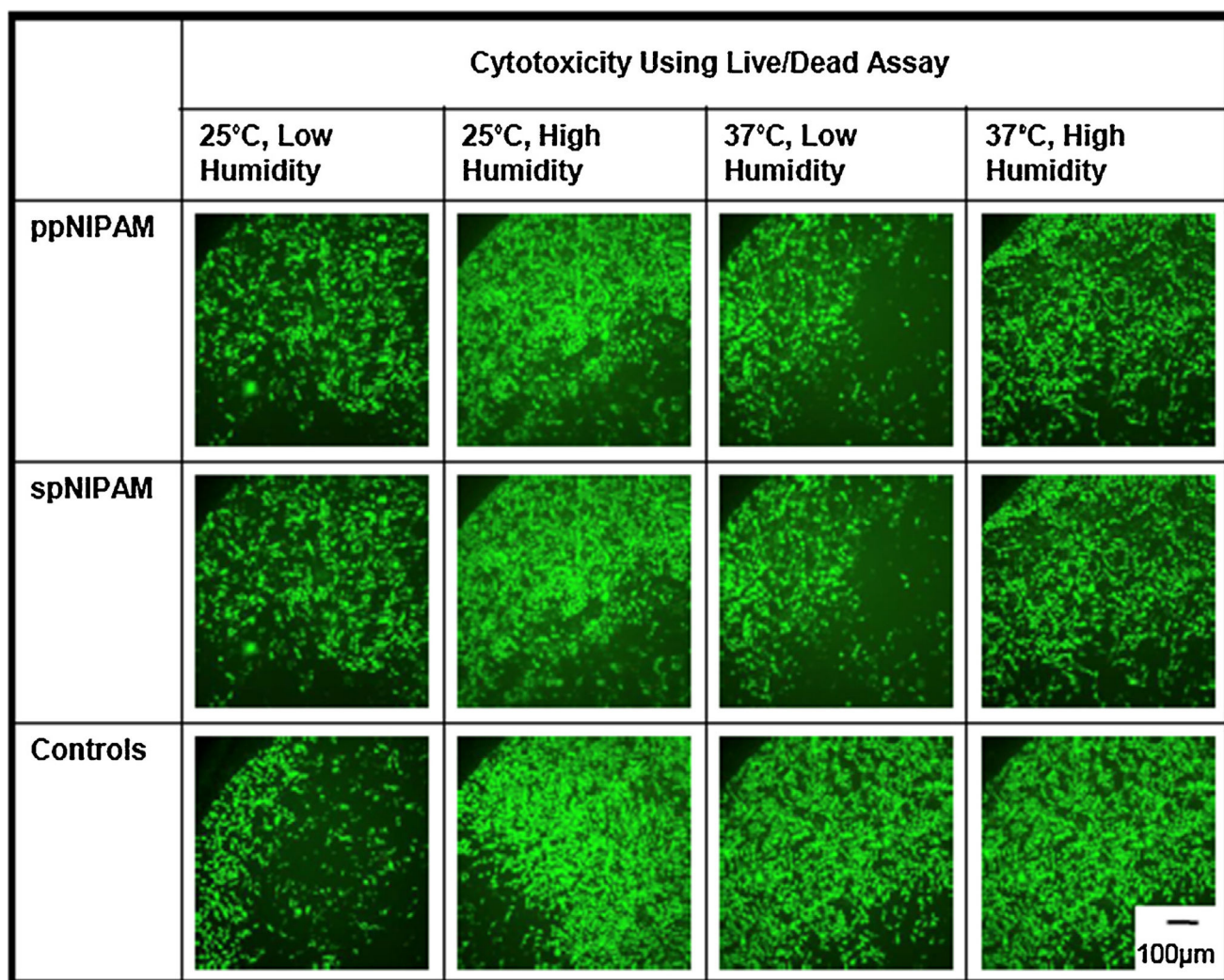


Fig. 4. Fluorescent microscopy images showing live (green) and dead (red) BAECs after 24 h of incubation with 100% treated media extracted from ppNIPAM (top), spNIPAM (middle), or blank control glass surfaces (bottom). All conditions maintained normal cell growth resulting in live cells after being exposed to treated media. (For interpretation of the references to colour in this figure legend, the reader is referred to the web version of this article.)

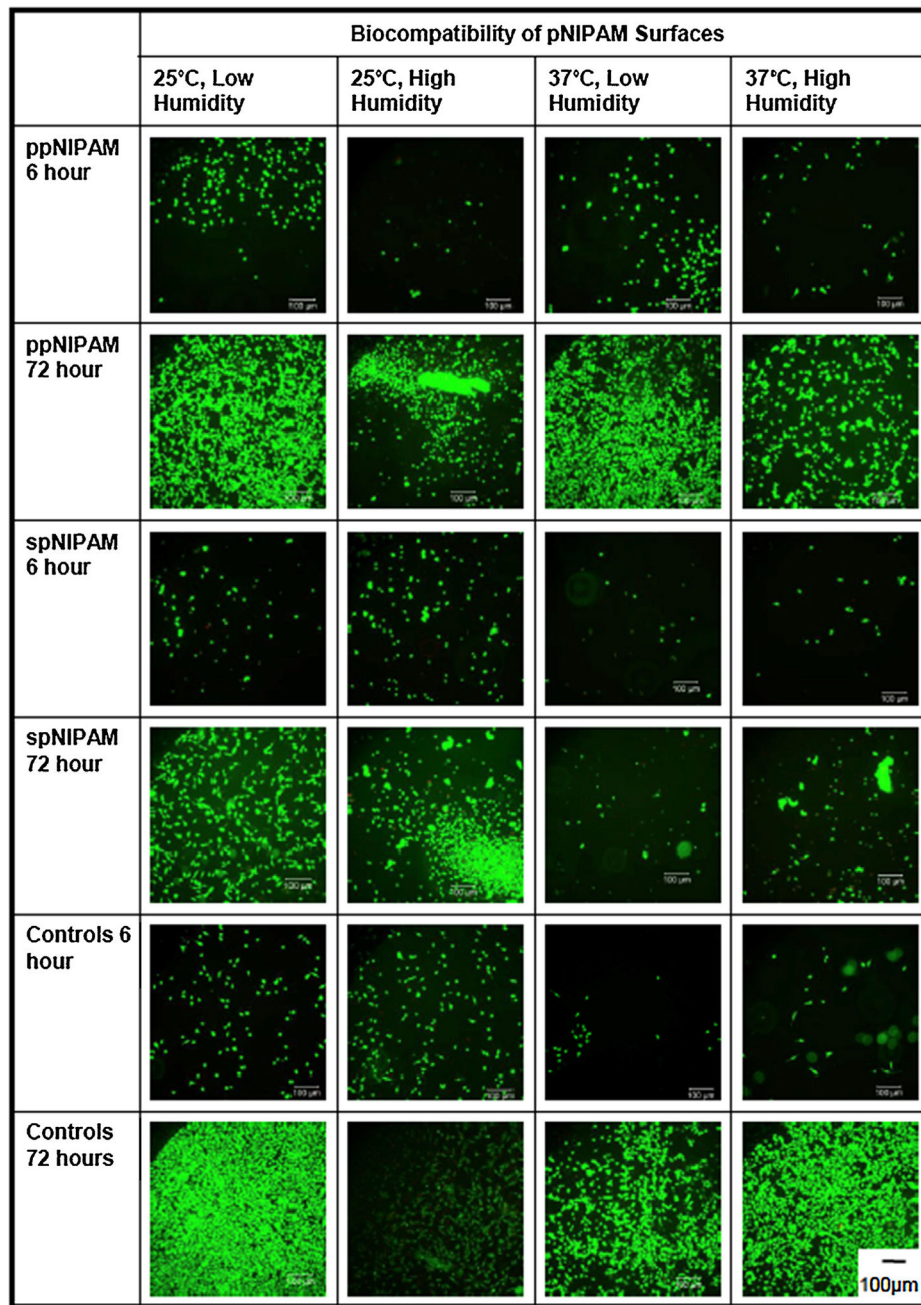


Fig. 5. Fluorescent microscopy images of BAECs on ppNIPAM (top), spNIPAM (middle), and control (bottom) surfaces during the biocompatibility study at 6 and 72 h of exposure to the surfaces. Cells attached and proliferated most on ppNIPAM surfaces.

Table 1

XPS survey data of ppNIPAM (top), spNIPAM (middle), and blank control Si chips (bottom) stored at 25°C low humidity (left), 37°C low (middle) and high humidity (right) conditions before submersion in DPBS for 0 (white), 2 (light grey), or 48 (dark grey) hours. PpNIPAM surfaces remained stable regardless of storage conditions. SpNIPAM surfaces were not stable over time, and the storage conditions affected the final surface composition. Surfaces stored at 25°C were more similar to the theoretical values obtained from the monomer composition by 48 h, where as surfaces stored at 37°C were similar to the control surfaces. N = 9 and the standard deviation was below 5 for each value reported above.

	XPS Survey: Relative Atomic Percent															
	25°C Low Humidity					37°C Low Humidity					37°C High Humidity					
	C	N	O	Si		C	N	O	Si		C	N	O	Si		
Theoretical Composition	75	12.5	12.5	0	75	12.5	12.5	0	75	12.5	12.5	0	75	12.5	12.5	0
ppNIPAM 0hr	78.4	8.7	12.8	0	77.8	11.0	11.2	0	79.4	10.6	9.7	0.2				
ppNIPAM 2hr	77.7	8.0	14.4	0	77.9	10.0	12.1	0	79.2	10.7	9.8	0.3				
ppNIPAM 48hr	76.0	10.4	13.6	0	75.8	10.3	13.9	0	79.3	10.9	9.7	0.2				
spNIPAM 0hr	33.5	5.0	43.3	18.2	37.4	5.6	40.1	16.9	34.7	5.0	41.9	18.3				
spNIPAM 2hr	59.3	8.7	23.8	8.2	61.6	9.3	22.5	6.7	58.3	8.7	23.5	9.5				
spNIPAM 48hr	28.3	4.1	47.6	20.0	22.8	2.9	52.4	21.9	22.8	2.1	52.1	22.9				
Control 0hr	11.0	0	42.3	46.7	11.0	0	42.3	46.7	11.0	0	42.3	46.7				
Control 2hr	11.2	0	40.5	48.3	13.8	0	41.6	44.7	13.9	0	43.1	43.1				
Control 48hr	15.2	0	52.7	32.1	19.7	0	50.5	29.8	14.9	0	56.1	29.1				

Table 2

XPS High Resolution Carbon data of ppNIPAM (top) and spNIPAM (bottom) stored at 25°C low humidity (left), 37°C low (middle) and high humidity (right) conditions before submersion in DPBS for 0 (white), 2 (light grey), or 48 (dark grey) hours. All surfaces maintain carbon binding environments indicative of pNIPAM deposition, regardless of storage conditions. N = 9 and the standard deviation was below 5 for each value reported above.

	High Resolution Carbon: Relative Atomic Percent											
	25°C Low Humidity				37°C Low Humidity				37°C High Humidity			
	CH/CC 285eV	CO/CN 286eV	O=CN 288eV	O=CN 288eV	CH/CC 285eV	CO/CN 286eV	O=CN 288eV	O=CN 288eV	CH/CC 285eV	CO/CN 286eV	O=CN 288eV	O=CN 288eV
Theoretical Composition	66.7	16.7	16.7	16.7	66.7	16.7	16.7	16.7	66.7	16.7	16.7	16.7
ppNIPAM 0hr	62.1	20.8	17.1	17.1	69.8	19.8	10.4	10.4	52.2	28.4	19.4	19.4
ppNIPAM 2hr	54.7	27.0	18.3	18.3	62.2	24.6	13.3	13.3	53.2	28.6	18.3	18.3
ppNIPAM 48hr	62.8	20.4	16.7	16.7	64.1	22.1	13.8	13.8	66.8	23.8	9.4	9.4
spNIPAM 0hr	68.7	17.1	14.2	14.2	62.1	20.2	17.7	17.7	65.1	20.2	14.7	14.7
spNIPAM 2hr	63.6	22.4	14.0	14.0	60.0	23.3	16.7	16.7	64.3	24.5	11.1	11.1
spNIPAM 48hr	72.4	13.2	14.4	14.4	60.6	23.4	15.9	15.9	62.2	22.3	15.5	15.5

Contact angles for ppNIPAM (top), spNIPAM (middle), and blank control surfaces (bottom) at all storage conditions taken above and below the LCST. Control surfaces show no thermoresponse, while ppNIPAM and spNIPAM surface before submerston in DPBS (0hr) were thermoresponsive.

Table 3

	Contact Angle							
	25°C Low Humidity		25°C High Humidity		37°C Low Humidity		37°C High Humidity	
	25°C	37°C	25°C	37°C	25°C	37°C	25°C	37°C
ppNIPAM 0hr	31.7 $\sigma=6.1$	42.2** $\sigma=3.8$	36.4 $\sigma=7.4$	42.6** $\sigma=5.9$	32.0 $\sigma=3.3$	43.4** $\sigma=5.8$	35.3 $\sigma=3.8$	43.5** $\sigma=4.7$
ppNIPAM 2hr	35.2 $\sigma=2.6$	39.4* $\sigma=1.3$	36.6 $\sigma=8.3$	43.4** $\sigma=5.9$	35.6 $\sigma=4.5$	42.7** $\sigma=1.3$	33.8 $\sigma=2.8$	42.7** $\sigma=4.3$
ppNIPAM 48hr	36.7 $\sigma=4.6$	43.4** $\sigma=2.3$	36.0 $\sigma=2.8$	43.7** $\sigma=3.6$	34.6 $\sigma=4.2$	41.4** $\sigma=4.3$	36.6 $\sigma=4.4$	38.9 $\sigma=1.2$
spNIPAM 0hr	38.8 $\sigma=4.0$	45.3*** $\sigma=2.3$	42.3 $\sigma=5.8$	47.8*** $\sigma=4.3$	42.9 $\sigma=6.2$	47.9* $\sigma=3.0$	40.0 $\sigma=3.9$	48.8** $\sigma=5.4$
spNIPAM 2hr	42.3 $\sigma=5.3$	45.3* $\sigma=4.0$	40.0 $\sigma=3.1$	43.3*** $\sigma=2.8$	41.5 $\sigma=5.5$	44.5* $\sigma=5.1$	40.6 $\sigma=2.8$	45.3** $\sigma=2.0$
spNIPAM 48hr	40.9 $\sigma=2.8$	41.1 $\sigma=4.3$	40.3 $\sigma=1.7$	42.0 $\sigma=3.9$	41.3 $\sigma=2.0$	35.1 $\sigma=1.4$	38.5 $\sigma=3.5$	34.7 $\sigma=1.7$
Control 0hr	44.8 $\sigma=1.7$	47.3 $\sigma=2.8$	43.9 $\sigma=3.3$	46.9 $\sigma=2.1$	45.3 $\sigma=5.4$	48.7 $\sigma=4.0$	44.5 $\sigma=6.7$	48.5 $\sigma=5.6$
Control 2hr	52.7 $\sigma=6.5$	54.8 $\sigma=5.7$	49.3 $\sigma=5.1$	51.2 $\sigma=4.5$	47.1 $\sigma=4.4$	51.5 $\sigma=6.9$	51.1 $\sigma=11.6$	52.9 $\sigma=5.5$
Control 48hr	30.5 $\sigma=8.6$	30.4 $\sigma=7.3$	25.2 $\sigma=3.3$	28.7 $\sigma=5.3$	26.7 $\sigma=3.3$	28.2 $\sigma=3.5$	26.1 $\sigma=3.0$	25.3 $\sigma=3.0$

PpNIPAM surfaces maintained thermoresponse after 48 h in DPBS, while spNIPAM surfaces showed either no thermoresponse or reverse thermoresponse. N = 9, samples marked with ** are very statistically significant (p < 0.006), * statistically significant (p < 0.05), and ■ are statistically significant (p < 0.05) but exhibit a reversed thermoresponse.